



**ARTICLE**

# Development and Field Application of Phosphogypsum-Based Soil Subgrade Stabilizers

Hongfei Yue<sup>1</sup>, Aiguo Fang<sup>2</sup>, Sudong Hua<sup>1,\*</sup>, Zenghuan Gu<sup>3</sup>, Yu Jia<sup>1</sup> and Cheng Yang<sup>4</sup>

<sup>1</sup>College of Materials Science and Engineering, Nanjing Tech University, Nanjing, 211800, China

<sup>2</sup>China Construction Installation Engineering Co., Ltd., Nanjing, 210023, China

<sup>3</sup>Jiangsu Subote New Material Co., Ltd., Nanjing, 211103, China

<sup>4</sup>Sinoma Construction Co., Ltd., Suzhou, 215300, China

\*Corresponding Author: Sudong Hua. Email: huasudong@126.com

Received: 23 August 2021 Accepted: 11 October 2021

## ABSTRACT

A phosphogypsum-based subgrade stabilizer (PBSS) was formulated using industrial by-product phosphogypsum (PG), mixed with slag and calcium-silicon-rich active material (GSR). The active powder (AP) was used to modify PBSS, and PBSS-AP was obtained. PBSS and PBSS-AP were each mixed with 10% silty soil, and cement and lime (CAL: 5% lime + 2% cement) were used as the traditional material for comparative experiments. Samples were cured under standard conditions, and tested for unconfined compressive strength (UCS), water stability, volume expansion, and leachate, to explore the stabilization effect of the three solidified materials on silty soil. The results showed that the comprehensive performance of silty soil mixed with 12% PBSS-AP was the best. The CaO, SiO<sub>2</sub> and Al<sub>2</sub>O<sub>3</sub> provided by PG, Slag and GSR will react with water to form a stable C-S-H gel, which is conducive to stabilizing the soil. Field application results showed that the compaction exceeded 95%, the deflection was 144.9 mm, and UCS was 2.5 MPa after 28 days. These findings indicated that PBSS-AP is an effective stabilizer for subgrade soils.

## KEYWORDS

Phosphogypsum; solidified material; unconfined compressive strength; water stability; volume expansion; leachate

## 1 Introduction

Phosphogypsum (PG), a by-product of industrial production of phosphoric acid and phosphate fertilizer, has a unique characteristic where it swells after absorbing water [1]. The annual global production of PG is approximately 100–280 million tons [2–4]. The rate of PG utilization is low compared to that of other industrial wastes, owing to the fact that phosphogypsum swells after absorbing water, and also contains dangerous elements [5]. Nevertheless, previous studies have shown that PG can be used in the manufacture of cement admixtures, mortars, sulphuric acid, soil improvers, and salts [6–10]. Although, the amount of PG used in production of these products is relatively small, it is challenging to overcome its large accumulation [7,11–13]. Consequently, PG now occupies large amounts of land areas that could otherwise be used for cultivation. When rainwater soaks into the ground, several harmful substances



penetrate, causing soil compaction and contaminating groundwater, thereby causing serious threats to people's lives [12].

Lime and cement are traditional soil subgrade stabilizers that are extensively used in road engineering, owing to their superior economic and excellent solidification effects [14–18]. However, production of lime and cement requires large amounts of natural raw materials, and the process emits large amounts of harmful exhaust gases, such as CO<sub>2</sub>, SO<sub>3</sub>, and NO<sub>x</sub> [19,20]. To protect the ecological environment and lower road construction cost, researchers are currently exploring use of industrial waste as a substitute for traditional cement and lime. For example, Mavroulidou [21] explored approaches to improve different clay properties of waste paper sludge [21], while Seslija et al. [22] used fly ash to replace natural materials as building materials. On the other hand, Etim et al. [16] used iron ore tailings and lime as soil conditioners to improve the properties of black cotton soil. Their results showed that these materials significantly reduced the environmental impact of iron ore tailings disposal, and the improved soil could be used as a low-flow roadbed material. Moreover, Reginald and Abir [23] explored the potential use of cement and lime-activated blast furnace slag in solidified mixed contaminated soils, by determined unconfined compressive strength and leaching toxicity.

The Chinese government's emphasis on the need for environmental protection has resulted in reduction in production and use of traditional road building materials that have high energy consumption and high emissions, such as lime and cement [24–26]. Since the demand for raw materials in road engineering remains high, researchers have shifted attention onto PG as an alternative material to cement and lime, with the aim of increasing its industrial-scale consumption opportunities. In fact, PG can solve the problem of excessive cost of traditional materials in road construction. Since its first use in road engineering in the USA in 1980, analytical results have shown that PG mixed with soil results in a stable structure [2]. To date, however, only a handful of studies have explored the use of PG in large-scale road engineering, mainly because large amounts of PG have poor effects on soil pressure resistance and water stability [27]. For example, Ding et al. [5] reported that excessive use of PG in roads caused roadbeds and pavements to swell and form cracks. In addition, Tebogo et al. [3] explored the properties of soils solidified with large amounts of PG and other wastes. In the present study, the active material AP was used to modify PG, with the aim of improving the unconfined compressive strength, water resistance, and volume stability of phosphogypsum-based soil-solidified materials (PBSS). In addition, performance of the solidified materials after application in road construction was also evaluated.

## 2 Materials and Methods

### 2.1 Materials

#### 2.1.1 Soil

Silty soil from northern Jiangsu, China was used in the current study. The construction standards of a normal roadbed indicate that soil to be used should be mixed with that of solidified material under an optimal moisture content [28]. Prior to stabilization, the chemical composition of the silty soil was determined via X-ray fluorescence spectrometry. Results for specific test results are presented in Table 1, whereas results of the basic physical properties of the silty soil determined in accordance with the specifications of the Chinese GB/T 50123-1999, are shown in Table 2.

**Table 1:** Chemical composition of silty soil

Composition	SiO <sub>2</sub>	Fe <sub>2</sub> O <sub>3</sub>	Al <sub>2</sub> O <sub>3</sub>	TiO <sub>2</sub>	CaO	MgO	K <sub>2</sub> O	Na <sub>2</sub> O	P <sub>2</sub> O <sub>5</sub>	MnO	LOI
Content (%)	59.97	4.14	12.58	0.69	8.28	2.59	2.37	1.50	0.32	0.06	7.23

Note: R<sub>2</sub>O: alkali metal oxide; LOI: loss on ignition at 1000°C.

**Table 2:** Basic physical properties of silty soil

Basic nature	Specific gravity	Liquid limit (%)	Plastic limit (%)	Dry density Maximum (g/cm <sup>3</sup> )	Optimum moisture content (%)	Density (g/cm <sup>3</sup> )
Value	2.61	30	16	1.71	16	1.79

Results showed that SiO<sub>2</sub> (59.97%) was the main component of the silty soil, followed by Al<sub>2</sub>O<sub>3</sub> (12.58%), and CaO (8.28%) (Table 1). The silty soil had a specific gravity of 2.61 g/cm<sup>3</sup>, with liquid and plastic limits of 30 and 16%, respectively, and an optimum moisture content of 16% (Table 2).

### 2.1.2 Soil Stabilization Material

The main raw materials for preparation of PBSS included original PG, Calcium-silicon-rich active material GSR, and slag. Original PG is provided by Jiangsu Yuxing Chemical Industry Co., Ltd., China. GSR, and slag purchased from Suqian Huawo Building Materials Trading Co., Ltd., China. Lime and cement (CAL) are traditional soil-solidified materials used on roadbeds. Since the subgrade is likely to expand if the amount of lime in the subgrade is too high, used 2% and 5% cement and lime, respectively, in the soil [29,30]. The main chemical components of the original PG, Slag, and GSR based on X-ray fluorescence spectrometry are presented in Table 3.

**Table 3:** Chemical composition of raw materials

Material	SiO <sub>2</sub>	Al <sub>2</sub> O <sub>3</sub>	CaO	Fe <sub>2</sub> O <sub>3</sub>	SO <sub>3</sub>	MgO	TiO <sub>2</sub>	P <sub>2</sub> O <sub>5</sub>	LOI
PG	11.68	2.96	30.53	0.35	46.55	0.48	—	1.65	3.57
Slag	38.56	13.20	26.24	3.77	0.70	14.22	0.56	0.05	0.74
GSR	21.35	5.45	57.03	3.69	3.10	4.01	0.28	0.16	2.51

Note: R<sub>2</sub>O: alkali metal oxide; LOI: loss on ignition at 1000°C.

Next, explored the properties of the newly solidified material PBSS prepared using a large amount of industrial PG, and modified into PBSS-AP by adding AP. Results indicated that PBSS-AP could improve performance of solidified silty soil, thus ultimately meeting the roadbed requirements. The proportion of the original PG in PBSS was selected as 40% following several orthogonal and optimization experiments, and based on the compressive strength of the sample and amount of phosphogypsum used. In addition, used traditional CAL samples for comparative experiments to explore stability of PBSS in the subgrade soil. Since the newly solidified PBSS material comprised large amounts of PG, it was necessary to explore long-term stability of the cured sample. This included long-term analysis of samples solidified by three different materials, namely PBSS, PBSS-AP, and CAL. To this end, several tests including, analysis of UCS, water stability, volume stability, and toxicity of leachate, were performed.

### 2.1.3 Additives

The additive, AP, is an inorganic and silicon-rich powder developed to improve early strength of soil-solidified materials. The optimal proportion of AP in the present study was 5% of PBSS. The active material AP was thoroughly mixed with PBSS for 3 minutes during formulation of PBSS-AP to improve uniformity of contact between the additive and PBSS. See Table 4 for the AP chemical composition.

**Table 4:** Chemical composition of AP

Material	SiO <sub>2</sub>	Al <sub>2</sub> O <sub>3</sub>	CaO	Fe <sub>2</sub> O <sub>3</sub>	SO <sub>3</sub>	MgO	K <sub>2</sub> O	MgO	LOI
AP	91.34	1.25	1.45	1.32	0.31	1.14	1.02	—	2.17

Note: R<sub>2</sub>O: alkali metal oxide; LOI: loss on ignition at 1000°C.

## 2.2 Experimental Methods

### 2.2.1 Sample Preparation

Silty soil was first dried for 24 h, in a blast-drying oven at 80°C, to evaporate all water, then sieved to remove impurities. The solidified material was mixed with the silty soil for 30 s using a cement mortar mixer, distilled water added to the contents, followed by uniform mixing. The stirring continued for 3 min based on the optimal moisture content (slow stirring for 2 min, rapid stirring for 1 min). The resulting mixture had a maximum dry density and optimal moisture content of 1.67 g/cm<sup>3</sup> and 15%, respectively. A hollow cylindrical steel mold, with an inner diameter of  $\Phi$  50 mm  $\times$  50 mm, was used for sample preparation. The uniformly mixed mixture was first placed in a mold, and press-molded using a hydraulic jack. Thereafter, the sample was incubated in a standard curing box maintained at a temperature of 20  $\pm$  2°C, and relative humidity 90%.

### 2.2.2 Unconfined Compressive Strength (UCS)

Analysis of the sample UCS was divided into two parts. The first part entailed determination of the effect of different amounts of PBSS in the soil on the UCS value of the sample, while the second involved analyzing the effect of silty soil with different solidified materials (CAL, PBSS, and PBSS-AP) on the UCS value of the sample. The amount of PBSS and PBSS-AP in the soil was maintained at 10%, to avoid swelling due to excess phosphogypsum content and reduce application costs. The experimental method was based on the specifications of the Chinese standard JTG E51-2009, which is similar to ASTM D-2166. UCS of the sample was determined using WHY-200 microcomputer-controlled automatic compression tester.

### 2.2.3 Determination of Water Stability

Previous studies have shown that analysis of water stability is an indispensable test following completion of road subgrade construction, while the degree of damage to the roadbed after rainwater erosion can directly affect quality of the road [31,32]. In this study, the low-lying section of the road was immersed in water to simulate the effect of long-term rainy weather on the roadbed. The experiment was performed by immersing the prepared sample in a water tank for different periods of time and periodically observing the shape of the sample. The sample was taken out on day 3, 7, 28, and 60. Next, moisture on the surface of the sample was gently absorbed using a dry paper towel, and the sample weighed. The rate of water absorption  $R_w$  in the sample under different soaking times was calculated as follows:

$$R_w = \frac{G_2 - G_1}{G_1} \times 100\%$$

where  $R_w$  represents water absorption,  $G_1$  and  $G_2$  denote mass of the sample before and after immersion in water, respectively, at a specific time. The sample's UCS value was also determined after soaking. All water stability experiments were performed in accordance with the requirements of the Chinese standard JTG E51-2009.

### 2.2.4 Determination of Volume Stability

$\text{CaSO}_4 \cdot 2\text{H}_2\text{O}$  reacts with calcium oxide (CaO) and activated alumina ( $\text{Al}_2\text{O}_3$ ), after addition of PG to the soil, to produce hydrated calcium sulphoaluminate (generally referred to as ettringite), which rapidly explodes when exposed to water, thereby causing significant damage to the road bed and surface [27]. In the present study, the rate of volume expansion in the sample was determined according to the guidelines in the Chinese Standard GB/T 50123-1999, with the aim of determining variations in sample volume following addition of the three different solidified materials to silty soil.

### 2.2.5 Leachate Test

A Leachate test was performed according to the latest Chinese Standard HJ 557-2010. Specifically, the cured sample at a certain age was first crushed and passed through a sieve (with a 3 mm aperture), then 100 g of the sieved sample particles mixed with 1000 ml of deionized water in a clean plastic bottle. The oscillation frequency of the horizontal oscillator was adjusted to  $100 \pm 10$  times/min with an amplitude of 40 mm. Next, the leachate was shaken at room temperature for 8 h, and let to stand on the bench for 16 h. Finally, the supernatant was filtered through a  $0.45 \mu\text{m}$  microporous membrane, and the filtered leachate collected for testing.

### 2.2.6 Microscopic Analysis

A scanning electron microscope (SEM) (JEOL, JSM-5900, Japan) was used to examine the surface topography of pure PBSS and PBSS-AP paste-hardened bodies. Differences in surface and structure between them were then compared.

## 3 Laboratory Test Results

### 3.1 Unconfined Compressive Strength

UCS results across test samples at different ages, after addition of different soil solidified materials, are presented in Fig. 1. Summarily, the proportion of PBSS and PBSS-AP was maintained at 10%, whereas the traditional lime-cement system comprised 5% lime and 2% cement. Moreover, the UCS of the sample doped with the PBSS material was significantly higher than that of conventional lime-cement material (Fig. 1). The early strength of the PBSS-AP sample was also significantly improved. The UCS of the PBSS-AP sample at 7 days was approximately 4 MPa, whereas that in the sample with Lime-cement was approximately 2 MPa. Notably, the late strength of the PBSS sample was the most significant, increasing from less than 3 MPa at 7 days of curing to more than 4 MPa after 28 days. No significant changes in UCS value of the lime-cement sample during a similar period, with 2.5 MPa recorded after 28 days of curing. The UCS of the PBSS-AP sample showed only a slight increase in the later period due to the high strength in the early period.

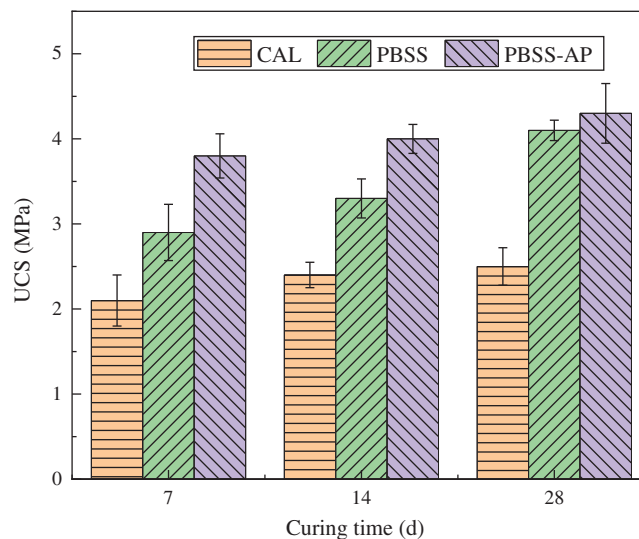


**Figure 1:** Effect of different soil stabilizing materials on UCS (means and standard deviations)

Changes in UCS, after addition of different amounts of PBSS, are shown in Fig. 2. Summarily, UCS increased from 3.2 MPa after 7 days of curing, to 4.4 MPa at day 28, when PBSS proportion was increased to 15%. However, the increase in UCS was not statistically significant relative to that observed in samples with 10% PBSS over the same period.

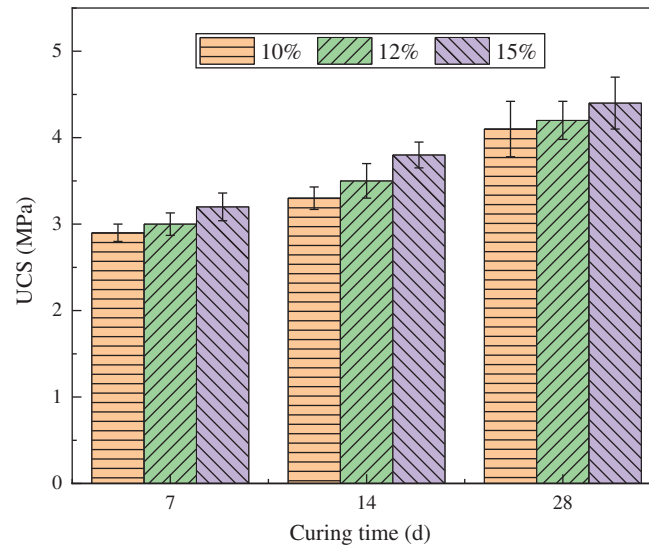


**Figure 2:** Effect of different PBSS dosage on UCS (means and standard deviations)

### 3.2 Water Stability

Samples mixed with lime and cement had lower weights than those from PBSS and PBSS-AP under similar conditions (Fig. 3). This was mainly attributed to the fact that PBSS and PBSS-AP samples were continuously absorbing water from a hydration reaction to produce a structurally stable hydrated calcium aluminate (C-A-H) [5]. However, CAL had a more stable hydration reaction, and a lower UCS value than those obtained in PBSS and PBSS-AP samples.

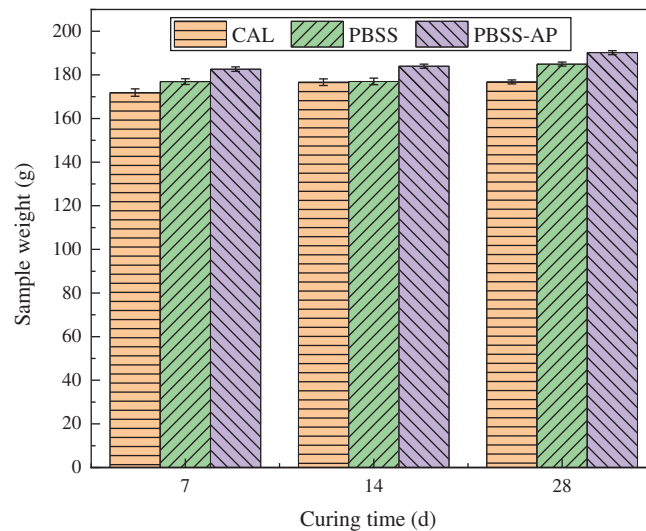


**Figure 3:** Weight of samples with different stabilizing materials at different times (means and standard deviations)

Lime-cement samples had a significantly higher water absorption rate than PBSS and PBSS-AP under different times (Figs. 4 and 5), mainly because the lime inside lime-cement samples required more water to decompose [33]. Notably, PBSS and PBSS-AP samples became denser due to the hydration reaction, and water molecules were not easily accessible. Apart from the sample's special structure, another reason for

the higher absorption rate may be that water molecules continuously gained entry to the inside of the sample for the hydration reaction. Furthermore, the sample had a lower water absorption rate after 28 days of curing than at 7 days. The rate of water absorption for PBSS-AP sample immersed in water was 7.3% after 3 days, and 8.2% after 60 days. Notably, no statistically significant differences in this change, mainly because the internal reaction of the sample ended after 28 days [34]. In addition, PBSS-AP modified sample had a stronger hydration reaction capacity, which made it to have a higher water absorption rate than that of the PBSS sample.

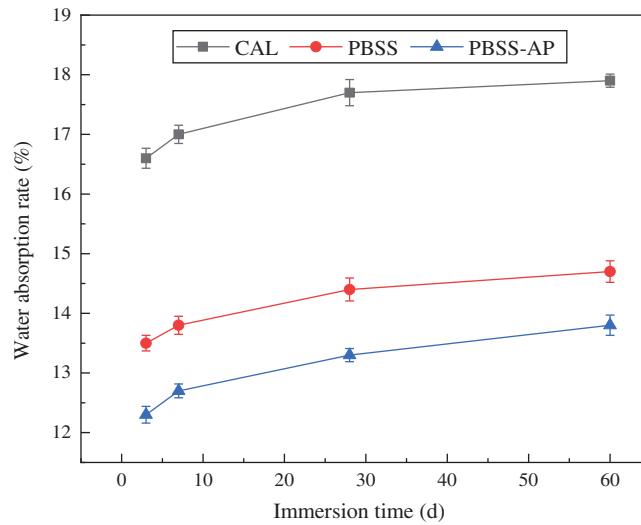


**Figure 4:** Water absorption rate of different samples after 7 days curing

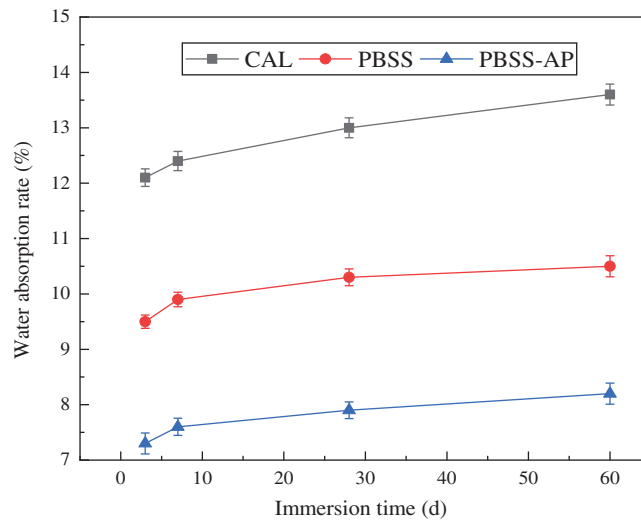


**Figure 5:** Water absorption rate of different samples after 28 days curing

The UCS values of all samples were significantly lower after 7 days of immersion curing, following which the trend showed an increase (Fig. 6). The CAL, PBSS, and PBSS-AP samples immersed for 3 days had UCS values of 1.2, 1.7, and 2.5 MPa, respectively. This is because the strength of the sample in the standard environment was mainly provided by the soil itself and the product of the hydration reaction of the solidified material. Specifically, water molecules gradually entered the sample after immersion in water, thereby destroying the soil structure, and reducing strength. However, hydration of

the solidified material increased with increase in soaking time, which gradually enhanced sample strength. In addition, both PBSS and PBSS-AP samples had stronger water resistance effects than lime-cement samples, mainly due to decomposition of lime in the lime-cement samples after water absorption [33]. The water molecules entered the inside, and damaged the structural stability of the samples.

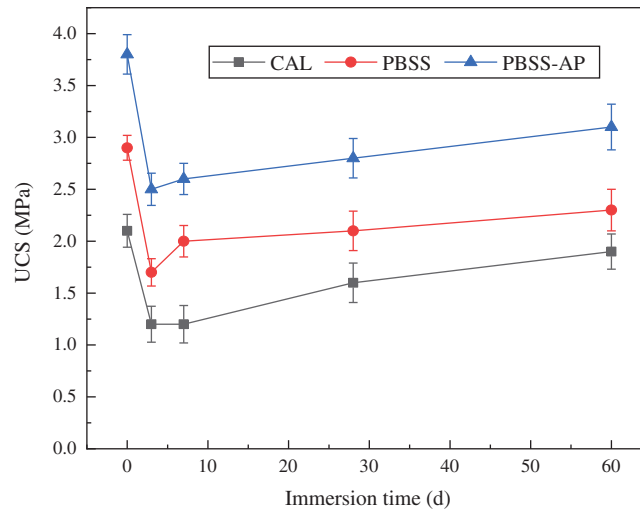


**Figure 6:** Trends in UCS values of the samples after immersion (samples cured for 7 days)

Profiles of UCS values of samples cured for 28 days and the corresponding trends after immersion in water are shown in Fig. 7. Summarily, samples cured for 28 days had higher water resistance than those cured for 7 days. In addition, CAL, PBSS, and PBSS-AP samples had UCS values of 1.3, 2.2, and 2.4 MPa, respectively, after 3 days of immersion in water. Notably, a slight increase in UCS was observed with increase in immersion time, mainly because the hydration reaction of the solidification material was completed after 28 days [34], which stabilized the UCS value.

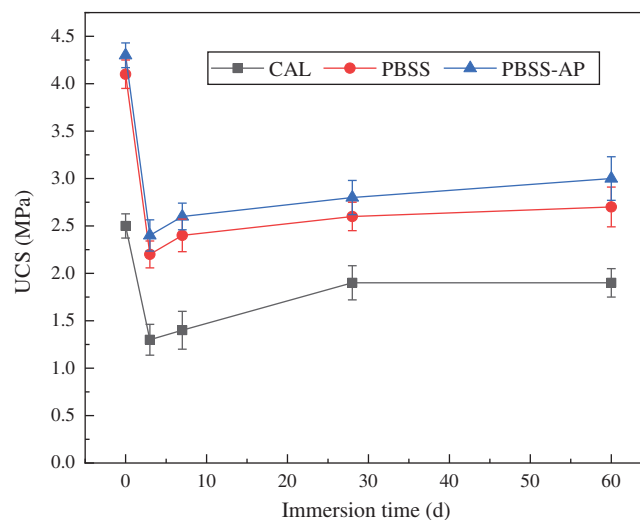


**Figure 7:** Trends in UCS values of the samples after immersion (samples cured for 28 days)

### 3.3 Volume Stability

Results showed that the PBSS sample had poor volume stability, while its expansion rate rapidly increased from 0.01% to 0.09% after 10 h and 240 h of water immersion, respectively (Fig. 8). In addition, CAL (0.08%) and PBSS-AP (0.06%) samples exhibited a relatively slow increase in expansion rate after immersion in water for 240 h. However, the PBSS-AP sample had a significantly higher volume stability, mainly due to the accelerated hydration reaction rate of the solidified material inside the sample, which resulted in high early strength, stable structure, and reduced expansion of the sample. Continuous hydration reaction of the solidified material inside the sample, improved stability of the structure of the sample, and the volume of the three samples was stable after immersion for 500 h.

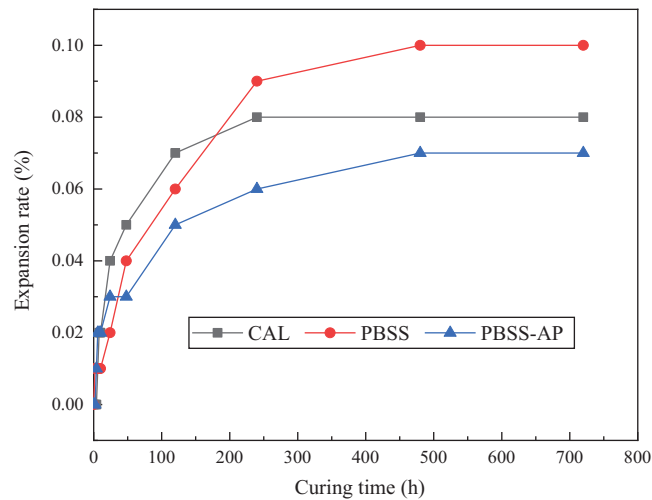


**Figure 8:** Relationship between sample volume expansion rate and time

Further analysis revealed presence of micro cracks on the surface of CAL samples, and these were significant after immersion in water for some time. Notably, PBSS-AP samples exposed to the same conditions had a better appearance (Fig. 9), indicating that use of PG as a solidifying material for the soil improved stability and expansion ratio. Notably, the PBSS-AP sample had a significantly lower expansion rate than PBSS, although this was still to that of the CAL sample. Overall, these results indicated that AP is a suitable solidification material for subgrade soil.

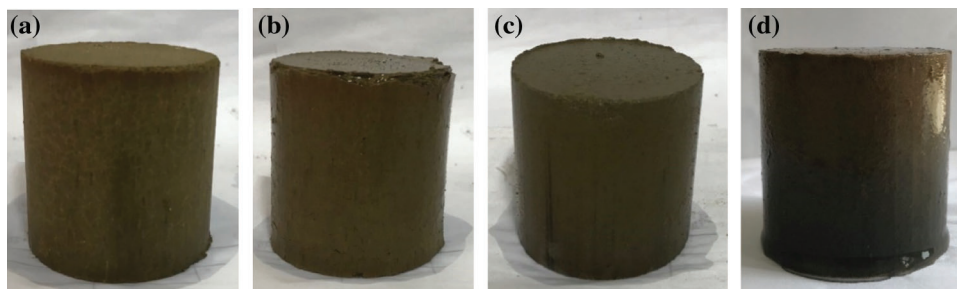


**Figure 9:** Appearance of samples under different curing conditions. (a) CAL cured for 28 days in a standard room; (b) CAL cured for 28 days in water; (c) PBSS-AP cured for 28 days in a standard room; (d) PBSS-AP cured for 28 days in water

### 3.4 Leachate Test

Results of the leachate test for PBSS-AP samples are presented in Table 5. Summarily, although PBSS-AP samples had several possible harmful elements, they were significantly lower than limits specified in the Chinese Standard GB 5085.3-2007. This indicates that use of PBSS-AP as a roadbed construction material does not pause a threat to the environment.

**Table 5:** Leachate test results of PBSS-AP samples

Element	Ba	Cr	Cu	Ni	Pb	Zn
Concentration (mg/L)	0.094	0.023	Nd	Nd	Nd	0.004
Limit (mg/L)	100	5	100	5	5	100

Note: Nd-not detected.

### 3.5 Microscopic Analysis

Used microscopy to explore differences between PBSS and PBSS-AP samples, targeting hardened bodies made from these two materials. Results are presented in Fig. 10.

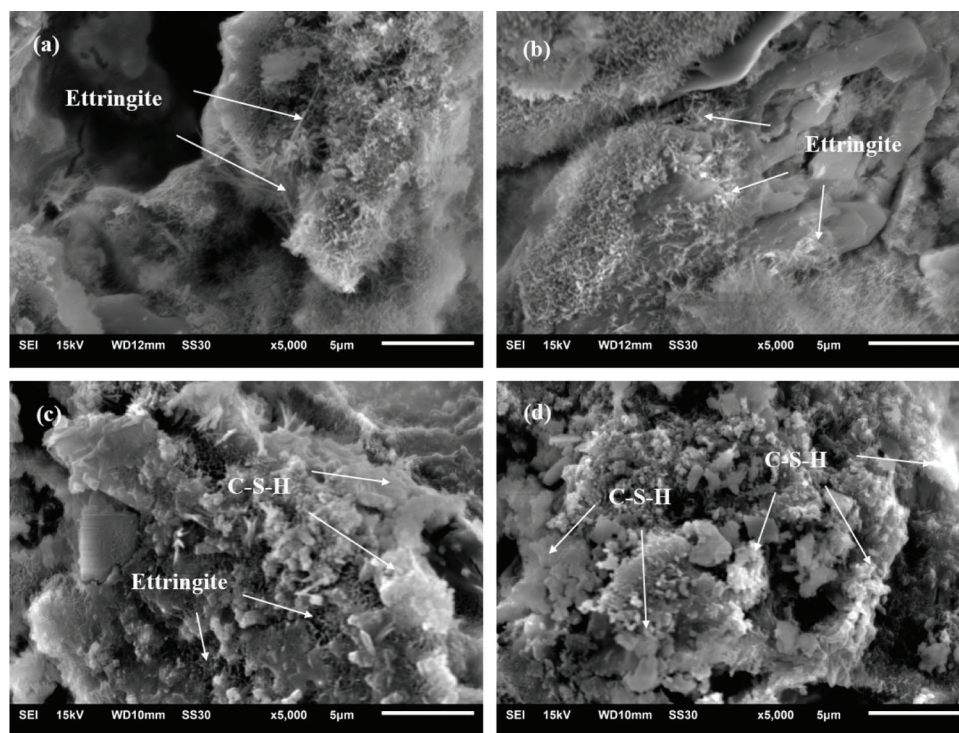


**Figure 10:** SEM images of PBSS and PBSS-AP hardened body: (a) PBSS cured for 3 days; (b) PBSS-AP cured for 3 days; (c) PBSS cured for 28 days; (d) PBSS-AP cured for 28 days

Results showed that no hydration reaction of PBSS and PBSS-AP was completed in the early stage, although more ettringite was formed at this stage (Fig. 10). However, it was found that significantly lower ettringite content and significantly higher hydrated product C-S-H content after 28 days. In addition, PBSS-AP had less ettringite content, denser hardened body, and higher strength than PBSS (Figs. 10c and 10d), indicating that it performed better in soil solidification [5].

#### 4 Field Application

To explore the practical application effect of the soil subgrade stabilizer material developed using industrial by-product PG, selected a provincial road under construction in the northern part of Jiangsu Province, China, for field testing. The study area has a warm temperate monsoon climate zone, while the basic landform type of the test section was that of the Xuhuai yellow floodplain area. The river is gentle, with no scouring, while its surface layer is mainly composed of silty soil. The area has soft soil, falls into category IV, while its surface water is slightly corrosive to reinforced concrete structures.

Specifically, PBSS-AP was used as the solidified material for field testing, with a dosage set to 12%. The test section was the K2+500-K2+720 left non-motor vehicle road base of the provincial road reconstruction project. The test section parameters were designed as: 30 cm, 12% PBSS-AP treatment soil (compaction degree  $\geq 88\%$ ) + 30 cm, 12% PBSS-AP treatment (compaction degree  $\geq 93\%$ ) + 20 cm, and 12% PBSS-AP treatment (compaction degree  $\geq 96\%$ ). In addition, selected top and bottom width of the non-motorized roadbed to be 6.71 and 7.91 m, respectively, then divided the section into three layers (including a base layer), with a slope of 1:1.5. Profile of the design layer is presented in Fig. 11, while the main construction process is illustrated in Fig. 12.

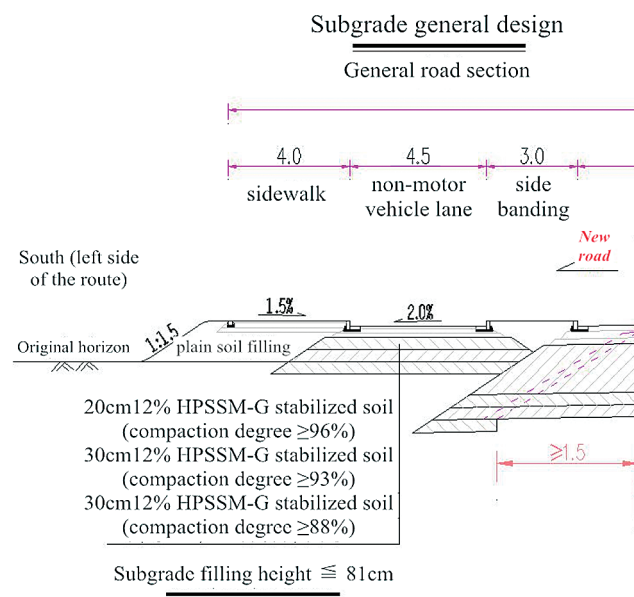


**Figure 11:** Sectional view of the subgrade design layer

The test section was first cured for two days, according to the project schedule, then local quality inspection department personnel invited to analyze performance of the roadbed, including compaction and deflection. Final test results revealed that the lower, upper and base layer beds had 95%, 95% and 97% compaction rates, respectively (Table 6). Moreover, the surface had a deflection of 144.9 mm (Table 7), while its UCS value reached 2.5 MPa after 28 days (Table 8).

Results from on-site inspection showed that all the data met the requirements, and reliability of PBSS-AP in road engineering (subbase + roadbed) was preliminarily verified. To further explore the quality of the roadbed, leachate and roadbed deformation will be continuously tracked and monitored during the winter and summer of each year.



**Figure 12:** Field test specific construction process: (a) Mechanical paving; (b) Mechanical stirring; (c) Roller compaction and leveling; (d) Curing

**Table 6:** Test results of compaction degree

Detection site		Test items	Test results	Request/standard value	Remarks
Road bed	Upper road bed	Compaction degree	95%	$\geq 93\%$	Fulfil requirements
	Down road bed		95%	$\geq 88\%$	Fulfil requirements
Road surface	Subbase		97%	$\geq 96\%$	Fulfil requirements

**Table 7:** Test result of deflection value

Serial number	Detection section	Total number of test points	Deflection average (0.01 mm)	Standard deviation (0.01 mm)	Deflection representative value (0.01 mm)	Technical indicators (0.01 mm)	Result determination
1	K1+540—K1+720 Left non-motor vehicle lane	20	99.8	22.57	144.9	$\leq 212.0$	qualified

**Table 8:** Test result of UCS

Curing time (d)	7	14	28
UCS (MPa)	1.5	2.0	2.5

## 5 Conclusion

In summary, soil samples with 10% PBSS had higher UCS values than those with CAL over a similar period. However, a 15% increase in PBSS caused a slight increase in UCS value after 28 days. The PBSS-AP sample showed a better stabilization effect, whereas the UCS values after 7, 14, and 28 days were 3.8, 4.0, and 4.3 MPa, respectively, which were significantly higher than those of PBSS and CAL samples.

The PBSS-AP sample had the most stable internal structure and the strongest water corrosion resistance, as evidenced by a higher UCS value relative to those obtained in PBSS and CAL samples at the same immersion period. Notably, the PBSS-AP sample had a UCS value of 3 MPa after 28 days of curing, and 60 days of immersion in water.

Results from Leachate test revealed that the PBSS-AP sample had a significantly lower concentration of harmful elements relative to the limit specified in the Chinese standard GB 5085.3-2007. In addition, field testing results, combined with the Chinese standard JTG D30-2015 and Chinese standard JTJ034-2000 requirements, showed that the main indicators (such as UCS, deflection, and compaction) of the roadbed solidified by PBSS-AP met the requirements for second-class roads in the People's Republic of China, whereas some of the indicators met the requirements for first-class roads. Taken together, these findings indicated that PG is suitable for largescale application in road construction.

**Data Availability:** Data used to support the findings of this study are available from the corresponding author upon request.

**Funding Statement:** This work was supported by funds from the Jiangsu Provincial Science and Technology Department's Social Development-Major Science and Technology Demonstration Project (Grant No. BE2018697), the Jiangsu Provincial Science and Technology Department Social Development Project (Grant No. BE2017704) and the Scientific Research Project of the Suqian Municipal Transportation Bureau.

**Conflicts of Interest:** The authors declare that they have no conflicts of interest to report regarding the present study.

## References

1. Liang, H. H., Li, J. L. (2015). The influence of hydration and swelling properties of gypsum on the preparation of lightweight brick using water supply reservoir sediment. *Construction and Building Materials*, 94(5), 691–700. DOI 10.1016/j.conbuildmat.2015.07.111.
2. Perez-Lopez, R., Macias, F., Ruiz Canovas, C., Miguel Sarmiento, A., Maria Perez-Moreno, S. (2016). Pollutant flows from a phosphogypsum disposal area to an estuarine environment: An insight from geochemical signatures. *Science of the Total Environment*, 553, 42–51. DOI 10.1016/j.scitotenv.2016.02.070.
3. Mashifana, T. P., Okonta, F. N., Ntuli, F. (2018). Geotechnical properties and microstructure of lime-fly ash-phosphogypsum-stabilized soil. *Advances in Civil Engineering*, 2018(5), 1–9. DOI DOI 10.1155/2018/3640868.
4. Gijbels, K., Hoang, N., Kinnunen, P., Schroyers, W., Pontikes, Y. et al. (2019). Feasibility of incorporating phosphogypsum in ettringite-based binder from ladle slag. *Journal of Cleaner Production*, 237, 117793. DOI 10.1016/j.jclepro.2019.117793.
5. Ding, J., Shi, M., Liu, W., Wan, X. (2019). Failure of roadway subbase induced by overuse of phosphogypsum. *Journal of Performance of Constructed Facilities*, 33(2), 04019013. DOI 10.1061/(asce)cf.1943-5509.0001278.
6. Yang, L., Zhang, Y., Yan, Y. (2016). Utilization of original phosphogypsum as raw material for the preparation of self-leveling mortar. *Journal of Cleaner Production*, 127, 204–213. DOI 10.1016/j.jclepro.2016.04.054.
7. Ennaciri, Y., El Alaoui-Belghiti, H., Bettach, M. (2019). Comparative study of K<sub>2</sub>SO<sub>4</sub> production by wet conversion from phosphogypsum and synthetic gypsum. *Journal of Materials Research and Technology-Jmr&T*, 8(3), 2586–2596. DOI 10.1016/j.jmrt.2019.02.013.
8. Folek, S., Walawska, B., Wilczek, B., Miskiewicz, J. (2011). Use of phosphogypsum in road construction. *Polish Journal of Chemical Technology*, 13(2), 18–22. DOI 10.2478/v10026-011-0018-5.

9. Degirmenci, N. (2008). Utilization of phosphogypsum as raw and calcined material in manufacturing of building products. *Construction and Building Materials*, 22(8), 1857–1862. DOI 10.1016/j.conbuildmat.2007.04.024.
10. Saeed, K. A., Kassim, K. A., Nur, H., Yunus, N. Z. M. (2015). Strength of lime-cement stabilized tropical lateritic clay contaminated by heavy metals. *KSCE Journal of Civil Engineering*, 19(4), 887–892. DOI 10.1007/s12205-013-0086-6.
11. James, J., Pandian, P. K. (2014). Effect of phosphogypsum on strength of lime stabilized expansive soil. *Gradevinar*, 66(12), 1109–1116.
12. Zhou, L. (2018). Preparation of calcium fluoride using phosphogypsum by orthogonal experiment. *Open Chemistry*, 16(1), 864–868. DOI 10.1515/chem-2018-0093.
13. Shen, Y., Qian, J., Huang, Y., Yang, D. (2015). Synthesis of belite sulfoaluminate-ternesite cements with phosphogypsum. *Cement and Concrete Composites*, 63(8), 67–75. DOI 10.1016/j.cemconcomp.2015.09.003.
14. Sirivitmaitrie, C., Puppala, A. J., Saride, S., Hoyos, L. (2011). Combined lime-cement stabilization for longer life of low-volume roads. *Transportation Research*, 2204(1), 140–147. DOI 10.3141/2204-18.
15. Anggraini, V., Asadi, A., Syamsir, A., Huat, B. B. K. (2017). Three point bending flexural strength of cement treated tropical marine soil reinforced by lime treated natural fiber. *Measurement*, 111(6), 158–166. DOI 10.1016/j.measurement.2017.07.045.
16. Etim, R. K., Eberemu, A. O., Osinubi, K. J. (2017). Stabilization of black cotton soil with lime and iron ore tailings admixture. *Transportation Geotechnics*, 10, 85–95. DOI 10.1016/j.trgeo.2017.01.002.
17. Mengue, E., Mroueh, H., Lancelot, L., Eko, R. M. (2017). Mechanical improvement of a fine-grained lateritic soil treated with cement for use in road construction. *Journal of Materials in Civil Engineering*, 29(11), 04017206. DOI 10.1061/(ASCE)MT.1943-5533.0002059.
18. Nisti, M. B., Saueia, C. R., Malheiro, L. H., Groppo, G. H., Mazzilli, B. P. (2015). Lixiviation of natural radionuclides and heavy metals in tropical soils amended with phosphogypsum. *Journal of Environmental Radioactivity*, 144(2), 120–126. DOI 10.1016/j.jenvrad.2015.03.013.
19. Yoon, S., Mun, K., Hyung, W. (2018). Physical properties of activated slag concrete using phosphogypsum and waste lime as an activator. *Journal of Asian Architecture and Building Engineering*, 14(1), 189–195. DOI 10.3130/jaabe.14.189.
20. Chen, J., Zhao, F., Liu, Z., Ou, X., Hao, H. (2017). Greenhouse gas emissions from road construction in China: A province-level analysis. *Journal of Cleaner Production*, 168, 1039–1047. DOI 10.1016/j.jclepro.2017.08.243.
21. Mavroulidou, M. (2018). Use of waste paper sludge ash as a calcium-based stabiliser for clay soils. *Waste Management & Research: The Journal for a Sustainable Circular Economy*, 36(11), 1066–1072. DOI 10.1177/0734242X18804043.
22. Seslija, M., Radovic, N., Vasic, M., Dogo, M., Jotic, M. (2017). Physicomechanical properties of fly ash applicable in road construction. *Journal of the Croatian Association of Civil Engineers*, 69(10), 923–932. DOI 10.14256/jce.1860.2016.
23. Kogbara, R. B., Al-Tabbaa, A. (2011). Mechanical and leaching behaviour of slag-cement and lime-activated slag stabilised/solidified contaminated soil. *Science of the Total Environment*, 409(11), 2325–2335. DOI 10.1016/j.scitotenv.2011.02.037.
24. Li, W., Gao, S. (2018). Prospective on energy related carbon emissions peak integrating optimized intelligent algorithm with dry process technique application for China's cement industry. *Energy*, 165(1), 33–54. DOI 10.1016/j.energy.2018.09.152.
25. Shan, Y., Liu, Z., Guan, D. (2016). CO<sub>2</sub> emissions from China's lime industry. *Applied Energy*, 166, 245–252. DOI 10.1016/j.apenergy.2015.04.091.
26. Zhang, X., Wu, L., Zhang, R., Deng, S., Zhang, Y. et al. (2013). Evaluating the relationships among economic growth, energy consumption, air emissions and air environmental protection investment in China. *Renewable and Sustainable Energy Reviews*, 18, 259–270. DOI 10.1016/j.rser.2012.10.029.
27. Shen, W., Zhou, M., Ma, W., Hu, J., Cai, Z. (2009). Investigation on the application of steel slag-fly ash-phosphogypsum solidified material as road base material. *Journal of Hazardous Materials*, 164(1), 99–104. DOI 10.1016/j.jhazmat.2008.07.125.

28. Ghorbani, A., Hasanzadehshooiili, H., Mohamumadi, M., Sianati, F., Salimi, M. et al. (2019). Effect of selected nanospheres on the mechanical strength of lime-stabilized high-plasticity clay soils. *Advances in Civil Engineering*, 2019(2), 1–11.
29. Wang, L., Roy, A., Seals, R. K., Byerly, Z. (2005). Suppression of sulfate attack on a stabilized soil. *Journal of the American Ceramic Society*, 88(6), 1600–1606. DOI 10.1111/j.1551-2916.2005.00304.x.
30. Ferreira, S. R., Paiva, S. C., Oliveira Morais, J. J., Viana, R. B. (2017). Expansion evaluation of a soil of the municipality of Paulista-PE improved with lime. *Materia-Rio de Janeiro*, 22(1), e11930. DOI 10.1590/s1517-707620170005.0266.
31. Chen, D. H., Scullion, T., Hong, F., Lee, J. (2012). Pavement swelling and heaving at state highway 6. *Journal of Performance of Constructed Facilities*, 26(3), 335–344. DOI 10.1061/(ASCE)CF.1943-5509.0000237.
32. Ahmed, A. (2013). Recycled bassanite for enhancing the stability of poor subgrades clay soil in road construction projects. *Construction and Building Materials*, 48(9), 151–159. DOI 10.1016/j.conbuildmat.2013.05.089.
33. Harichane, K., Ghrici, M., Kenai, S. (2012). Effect of the combination of lime and natural pozzolana on the compaction and strength of soft clayey soils: A preliminary study. *Environmental Earth Sciences*, 66(8), 2197–2205. DOI 10.1007/s12665-011-1441-x.
34. Taher, M. A. (2007). Influence of thermally treated phosphogypsum on the properties of Portland slag cement. *Resources Conservation and Recycling*, 52(1), 28–38. DOI 10.1016/j.resconrec.2007.01.008.